

IMPROVED PARAMETERS OF THE HYDROGEN-DEFICIENT BINARY STAR KS PERTõnu Kipper¹ and Valentina G. Klochkova²¹ *Tartu Observatory, Tõravere, 61602, Estonia; tk@aai.ee*² *Special Astrophysical Observatory RAS, Nizhnij Arkhyz, 369167, Russia; valenta@sao.ru***Abstract**

Using the high resolution spectra secured with the Nasmyth Echelle Spectrograph NES of the 6 meter telescope we analysed the hydrogen-deficient binary star KS Per. The atmospheric parameters derived are: $T_{\text{eff}} = 9500 \pm 300$ K, $\log g = 2.0 \pm 0.5$, and $\xi_t = 9.5 \pm 0.5$ km s⁻¹. The hydrogen deficiency is $\text{H/He} = 3 \cdot 10^{-5}$, iron abundance is reduced by 0.8 dex, nitrogen abundance is very high $[\text{N/Fe}] = 1.4$, but carbon and oxygen abundances are low. The star luminosity is $\log L/L_{\odot} = 3.3$. A complex absorption and emission structure of the Na I D doublet was revealed. We suggest that the emission component forms in the circumbinary gaseous envelope.

Key words: stars: atmospheres – stars: individual: KS Per**1. INTRODUCTION**

Studies of the hydrogen-deficient binaries are interesting as these objects could be the progenitors of type Ia (Iben & Tutukov, 1993; Parthasarathy et al. 2007) or type Ib (Uomoto 1986) supernovae. Only four hydrogen-poor close binaries (HdBs) are currently known, which indicates that these objects are very rare. The primary components in HdBs are hydrogen-poor low-gravity A–F stars transferring matter to a secondary star. The high luminosity is provided by their helium-burning shell around a CO core. Nature of more massive but less luminous secondaries is unclear since their spectra are detected only in far UV spectral region. The hydrogen-deficiency of HdBs is believed to be due to case BB mass transfer in a binary system where the primary loses mass for a second time as it evolves through He burning in shell (Delgado & Thomas 1981). The most famous star among HdBs is *v* Sagittarii. That star was the first one for which the spectra of both components were seen by Dudley & Jeffery (1990)

who deconvolved the IUE 115–320 nm spectra. They determined the orbits, the mass ratio and the minimum mass for the primary. Their results of the minimum mass indicate that ν Sgr could be a progenitor of SN Ib.

A semi-regular pulsating star KS Per (\equiv HD 30353 \equiv Bidelman's star) was also found to be markedly deficient in hydrogen and to be a spectroscopic binary (Bidelman, 1950), and so the member of this small group. The pulsations which cause the semiregular light variations with a period of about 30 days were found by Osawa, Nishimura & Nariai (1963).

KS Per is an optical counterpart of an IR-source IRAS 04453+4311 (its IRAS-fluxes are given in Table 1). Dudley & Jeffery (1993) modelled the star's infrared flux and estimated the effective temperature of its circumstellar dust $T_{\text{eff}} = 1100$ K. Presence of hot circumstellar dust indicates recent or current mass loss. Indeed, Parthasarathy et al. (1990) analysed UV spectra (IUE) of KS Per and found shortward-shifted stellar wind profiles of various species. The terminal velocity from NV, CIV and Si IV lines reaches -650 km s^{-1} . The Mg II doublet has P Cygni profile with $v_{\text{term}} = -415 \text{ km s}^{-1}$. Other lines show shifts about -200 km s^{-1} . The large blueshifts are presented also in optical region by the H α line in our spectra (Fig. 1).

Margoni et al. (1988) studied radial velocities of KS Per and combining their own data with the earlier published ones they determined the orbital period of 362.8 d, semiamplitude $K = 48 \pm 2 \text{ km s}^{-1}$, and mass function $F(m) = 3.6 \pm 0.4 \mathcal{M}_{\odot}$. Although the mass function is relatively high, they did not find any trace of the companion spectrum in the optical region.

The presence of highly ionized species (NV and CIV) together with the UV-excess in the flux shortward of 180 nm suggest that the companion is an early B-type star. The mass-function $F(m)$ values derived from the single-lined spectroscopic orbits suggest that the primaries of hydrogen-poor close binaries may have CO core masses about $1\text{--}1.3 \mathcal{M}_{\odot}$ with extended outer envelopes. They may be in the post-AGB phase (Parthasarathy et al. 2007). The secondaries may have masses $3\text{--}4 \mathcal{M}_{\odot}$. From the early observations of KS Per no radiation from the secondary was found. This led Zeldovich & Guseinov (1966) to suppose that it is a collapsed star.

Whether KS Per is a supergiant, as the spectroscopic criteria show, is not definitely known (Bidelman 1950). Bidelman found from the interstellar reddening $E(B-V) = 0.44$ the distance about 2 kpc which means that the star is rather luminous supergiant ($M_V \approx -5^m$).

Most of the hydrogen deficient stars are rich in carbon (see, for example, Kipper & Klochkova 2005, 2006), but KS Per is not despite its spectrum resembles that of R CrB stars. In order to obtain accurate chemical abundances we performed high resolution spectral observa-

tions covering large spectral region. The results are reported in the following.

2. SPECTRAL OBSERVATIONS AND REDUCTION

Our high resolution spectra ($R=60000$) were obtained with the Nasmyth Echelle Spectrograph NES (Panchuk et al. 2007) permanently located at the Nasmyth focus of Russian 6 meter telescope. The spectrograph was equipped with an image slicer (Panchuk et al. 2007). As a detector a CCD camera with 2048×2048 pixels ($15 \times 15 \mu\text{m}$, readout noise $7e^-$) produced by the Copenhagen University Observatory was used. The spectral regions 521–668 nm were registered on August, 31 2007 (JD 2454344) and 394–540 nm on September, 01 2007 (JD 2454345). The spectra cover 394–668 nm without gaps until 610 nm. To increase the signal to noise ratio 8 individual exposures with exposure time 1800 sec were obtained.

The spectra were reduced using the NOAO astronomical data analysis facility IRAF. The use of image slicer results in three parallel strips of spectra in each order. These strips are wavelength shifted. Therefore all strips were reduced separately, linearized in the wavelength and coadded. We checked the accuracy of this procedure (Kipper & Klochkova 2005) and found that the wavelengths of the terrestrial lines in the stellar spectrum were reproduced within a few 0.001 Å-s.

The spectra were radial velocity corrected due to the solar motion using IRAF task “rvcorrect”. After that all the spectra were coadded. The continuum was placed by fitting low order spline functions through the manually indicated points in every order.

3. SPECTRAL ANALYSIS

3.1. Radial velocity

For spectroscopic binaries the radial velocity is an important parameter. Based on our high S/N and high resolution spectra covering large wavelength interval the accurate radial velocity was measured for the observed orbital phase. First, the 8 lines listed by Margoni et al. (1988) were identified. From those the $H\delta$ line and a Mg II doublet were excluded due to serious blending. The remaining 6 lines provide a provisional radial velocity $-31.9 \pm 1.4 \text{ km s}^{-1}$. With this velocity the other lines were identified. Due to low continuous opacity the number of lines in *KS Per* spectrum is much larger than in normal stellar spectra making the blending of serious issue. Using the most symmetrical and presumably unblended Fe II lines (32 lines) the heliocentric radial velocity $v_{\odot} = -32.3 \pm 1.7 \text{ km s}^{-1}$ was determined. No dependence of V_r on line formation depth was found. To get the velocity relative to LSR the correction -5.08 km s^{-1} should be added.

The systemic heliocentric radial velocity of about $+3 \text{ km s}^{-1}$ was

found by Margoni et al. (1988). That velocity agrees with the pattern of Galactic plane rotation in direction of KS Per (Dame et al. 2001) for distances less than 1 kpc.

In Fig. 1 the very strong Na I D doublet is plotted in velocity scale. Danziger et al. (1967) have used these lines for finding the interstellar (IS) reddening towards KS Per assuming that the radial velocity of the IS line is about $+5 \text{ km s}^{-1}$. This is clearly not the case as in Fig. 1 the lines are blueshifted by more than 20 km s^{-1} . In Bidelman's paper (1950) these lines were found to be redshifted by about 25 km s^{-1} . This radial velocity variation shows that these lines are of circumstellar origin. Note the P Cygni profile of red wings. Emission components of the Na I D lines are at the nearly zero radial velocity which agrees with the systemic velocity. Therefore we propose that this emission forms in the circumbinary gaseous envelope.

3.2. Model atmospheres

Early estimates of chemical composition of KS Per by Wallerstein et al. (1967) and Nariai (1967) showed that the atmosphere is very hydrogen-poor $\text{H/He} \approx 10^{-4}$ (by number). The abundance of carbon compared to that of nitrogen is also low. Logarithmic abundances by numbers found by Wallerstein et al. (1967) were $\text{He}=11.6$, $\text{C}=6.2$, and $\text{N}=9.2$. Dudley & Jeffery (1993) have also found that carbon abundance in HDs is lower than in extreme helium stars.

Such hydrogen-deficient atmospheric models were computed in Armagh Observatory using the code STERNE (Jeffery et al. 2001). These models take into account both hydrogen-deficiency and metal-line blanketing. From Armagh Observatory database the He+N models grid *h00he99n003* was chosen for the present analysis (see the Web-address <http://star.arm.ac.uk>).

3.3. Atmospheric parameters

Spectral type of KS Per is A5Iap (SIMBAD database). For normal stars this would correspond to $T_{\text{eff}} = 8600 \text{ K}$ and $\log g = 2.0$. But, as Danziger et al. (1967) have noted, when the lines are greatly enhanced by low opacity, the approximate spectral type cannot be used to infer the effective temperature or absolute magnitude with high accuracy. Early estimate by Nariai (1963) using photometry and line blanketing data is $T_{\text{eff}} = 8400 \text{ K}$. The same author (Nariai 1967) found using hydrogen-deficient model atmospheres $T_{\text{eff}} = 11000 \pm 1000 \text{ K}$, $\log g = 1 \pm 1$, and $\xi_t = 18 \text{ km s}^{-1}$. At the same time Wallerstein et al. (1967) also analysed the star and found ionization temperature $T_{\text{ion}} = 10080 \text{ K}$. They let $T_{\text{ion}} = T_{\text{eff}}$. Danziger et al. (1967) used interstellar polarization and reddening and obtained for KS Per $T_{\text{eff}} = 10000 \text{ K}$, $\log g = 2.0$, $E(B - V) = 0.35$ and $M_V = -3.2^m$.

Dudley & Jeffery (1993) analysed all four hydrogen-deficient close

binaries modelling their flux distribution. The model atmospheres were calculated with the assumed abundances: $n_{\text{H}} = 0.0002$, $n_{\text{He}} = 0.998$, $n_{\text{C}} = 0.00007$, and $n_{\text{N}} = 0.02$. For *KS Per* they obtained parameters: $T_{\text{eff}} = 12500 \pm 500$ K, $E_{B-V} = 0.55 \pm 0.10$, and $d = 3.9$ kpc. Recently Pandey (2006) estimated $T_{\text{eff}} = 10500$ K, $\log g = 1.5$, and $\xi_t = 10$ km s⁻¹.

We started with this last estimate. Forcing the excitation and ionization equilibriae of Fe I and Fe II we ended up with $T_{\text{eff}} = 9500 \pm 300$ K and $\log g = 2.0 \pm 0.5$. For this procedure we were forced to extrapolate Armagh atmospheric models towards lower temperatures by 1000 K. For the microturbulent parameter we got somewhat different values for Fe I and Fe II 8.3 and 9.4 km s⁻¹ respectively. Other elements lines were best fitted with similar microturbulent velocity values. We adopted the weighted by the number of used lines mean microturbulent velocity $\xi_t = 9.5 \pm 0.5$ km s⁻¹. This is considerably lower value than 18 km s⁻¹ found by Nariai (1967). For *v Sgr* Leushin (2001) found $\xi_t = 8 \div 12$ km s⁻¹ depending on spectral region.

3.4. Hydrogen content

The hydrogen to helium ratio was estimated by Wallerstein et al. (1967) to be near $1 \cdot 10^{-4}$ and by Nariai (1964) $3 \cdot 10^{-4}$. Using the new Armagh hydrogen-deficient model atmospheres we synthesized the H β , H γ and H δ lines (the H β and H δ lines are shown in Fig. 4). According to these figures H/He is close to $2 \cdot 10^{-5}$. Using the fitting of measured equivalent widths we got from the H γ and H δ lines H/He = $3 \cdot 10^{-5}$, but from the H β line much less $2 \cdot 10^{-6}$. This indicates that the H β line is seriously filled with emission (see left panel of Fig. 4). Also the red wing of the H β line is also slightly in emission showing P Cygni like profile. The central parts of the H γ and H δ lines are also filled with emission as could be judged from Fig. 4 where the synthesized relatively deep Doppler cores were not observed. Note that the same peculiarities of the Balmer lines profiles were observed in the spectrum of the another HdB star *v Sgr* (Leushin 2001).

3.5. Abundances

The abundances of other elements were derived with the help of Kurucz's program WIDTH5 together with the Armagh hydrogen-deficient model atmospheres. The sources of oscillator strengths are indicated in the Table 2, where the results are listed. Measured equivalent widths of lines, used oscillator strengths and derived abundances are listed in Table 4. For most lines the oscillator strengths by Thevenin (1989, 1990) and for C, N and O the data by Wiese et al. (1996) were used.

When the hydrogen is no longer the most abundant element, the usual scale, where the logarithmic abundance of hydrogen is 12.00, is no more convenient. In WIDTH5 the abundances are determined relative to total number of atoms. In the extremely hydrogen-poor

case this is the number of He atoms which in logarithmic scale should be taken 11.54 if one wishes to normalize $\log \Sigma \mu_i \varepsilon(i) = 12.15$ as in the solar case.

The low hydrogen abundance and consequently low continuous opacity leads to very large number of lines in stars spectrum. This in turn makes difficult to find nonblended lines for abundance determinations and increases the errors. The errors indicated in Table 2 are due to differing results from different lines. The systematic errors due to errors in T_{eff} , $\log g$ and ξ_t , found by changing these parameters, are less than these indicated errors.

First of all, the results show that KSPer is metal poor with the mass fraction of Fe reduced by 0.8 dex in accord with Nariai (1967) finding that the abundances of metals are about $10^{-2} \div 10^{-3}$ times that of α Cyg. The abundance of He, checked using 5 He I lines, is 11.54 ± 0.23 . No CI or CII lines were reliably identified. Only a CI line at 477.174 nm, which in the solar spectrum is blended with a Fe I line, was measured providing C abundance of 7.5. This is less than the input abundance. The He abundance also provides a circumstantial evidence for low carbon abundance. If the input C abundance is raised by 0.3 dex, the needed He abundance should be raised by 0.1 dex. The oxygen abundance is also low. Nitrogen is enhanced by large amount indicating that the surface material is primarily CNO processed. The *s*-process produced elements seem to be enhanced but just at the amount not exceeding the determination errors which are comparatively large due to small number of used lines and heavy blending.

Recall that the star studied is an counterpart of an IR-source. For such an object with a dusty-gaseous circumstellar envelope one could expect that the chemical abundances pattern is modified by selective separation processes. For example, a part of Fe deficit could be caused by gas-dust separation. The position of the star very close to the Galactic plane and its proper motion permit us to propose that it belongs to Pop. I and has normal metallicity. The CNO-triad, zink and sulfur are unaffected by selective fractioning processes. Since the abundances of CNO may vary due to nuclear reactions in the course of the star's evolution, the behaviour of Zn and S are critical for finding the efficiency of selective depletion. According to Wheller et al. (1989) and Timmes et al. (1995) the Zn abundance varies together with the Fe abundance over a wide range of metallicity and could be used as criterion of initial star metallicity.

Unfortunately, when studying the abundance of Zn in KSPer we encountered the difficulties which we were not able to overcome. Two stronger Zn I lines at 481.054 and 636.235 nm were found at the wavelengths 481.010 and 636.165 nm corresponding to radial velocities -32.9 and -33.0 km s⁻¹. The measured equivalent widths 23.0 and 22.3 pm, however, correspond to abundances of 5.97 and 6.22 in the scale of Table 2, when the oscillator strengths by Biémont & Godefroid (1980) were used. Solar abundance of zinc is about 4.6. Therefore we sup-

posed that these lines do not belong to Zn I but we were not able to identify their origin.

We searched also for a weaker Zn I line at 472.216 nm and found a line at 472.152 nm with $W_\lambda = 1.3$ pm. This will give the abundance 4.32 of zinc. However, the corresponding radial velocity is -40.6 km s^{-1} , which is much too different from the mean found from other lines.

The relative abundance of volatile element sulfur [S/Fe] in the atmosphere of KS Per is within the errors close to the solar one. In order to verify additionally the possible depletion pattern we plotted relative abundances [El/Fe] from Table 2 versus condensation temperature T_{cond} (Lodders 2003) (Fig. 5). No significant relation between T_{cond} and abundances was found. Thus we do not see any trace of selective separation in the circumstellar envelope of KS Per.

In the other HdB ν Sgr iron was found to be slightly overabundant (Leushin 2001). But the position of ν Sgr in the Galaxy is completely different from KS Per.

3.6. Luminosity

Bidelman (1950) in his pioneering work estimated using spectroscopic criteria $M_V \approx -5^m$, $E(B - V) = 0.4$ and distance about 2 kpc for KS Per. But, as already noted, for greatly enhanced lines these estimates could have large errors. Danziger et al. (1967) estimated from polarization measurements and comparisons with neighboring stars $0.25 < E(B - V) < 0.45$ and distance modules $9.6 \div 11^m$. They found the same numbers from Na I D IS line intensities, but as it turned out, the Na I D doublet in KS Per spectrum is entirely of circumstellar (CS) origin (see sec. 3.1). The absence of IS lines is in accord with KS Per position in so called Auriga Gap with very few molecular clouds. In microwave frequencies there are no objects towards KS Per (Jardine 2008). Parthasarathy et al. (1990) estimated from width-luminosity relationship of Mg II k emission line $M_V = -4 \div -6^m$, and $0.30 < E(B - V) < 0.45$ in according with Danziger et al. (1967). This means that $E(B - V) \approx 0.35$ is fairly well established.

The systemic heliocentric radial velocity of KS Per is about $+3 \text{ km s}^{-1}$ (Margoni et al. 1988) or $v_{\text{LSR}} = 0$. This means that the distance to KS Per is probably less than 1 kpc as the velocities due to galactic rotation in that direction are negative. According to Dame et al. (2001) the CO emission in direction of KS Per has a zero velocity component corresponding to local gas.

According to numerical code for galactic extinction by Hakkila et al. (1997) A_V reaches 1.5 ± 0.4 already at the distance 1 kpc. With $R \sim 3.1$ this corresponds to $E(B - V) = 0.48$ indicating that the distance should be less than 1 kpc. Therefore we end up with the estimate $M_V \approx -3.3^m$ and $\log L/L_\odot \approx 3.3$.

5. CONCLUSION

We have found that the chemical composition of metal- and hydrogen-deficient pulsating star KS Per corresponds to the material which is primarily CNO processed without indications of triple- α processing. During the CNO processing nitrogen is enhanced at the expense of carbon and oxygen. This happens during the first and second dredge-up and one could not decide whether the star has passed the second dredge-up. Soon after that the star will burn He sporadically via the triple- α process. The low carbon abundance shows that the donor star had not yet experienced the third dredge-up. In this sense it differs from the other group of hydrogen-poor stars – extreme helium stars (EHes) in which the carbon abundance is considerably enhanced.

Abundances in KS Per are quite close to the ones in its sibling ν Sgr except the abundance of neon and iron. In KS Per the Ne abundance is nearly normal but in ν Sgr it is greatly enhanced (Leushin et al. 1998). This indicates that KS Per is in somewhat earlier evolutionary phase than ν Sgr.

In Table 3 we compare the abundances in KS Per with the ones in a cool extreme helium star LS IV-14°109 with close atmospheric parameters ($T_{\text{eff}} = 9500$ K, $\log g = 0.9$ and Fe abundance) (Pandey et al. 2001)). Chemical abundances pattern of KS Per as a whole, with the exception of CNO-group, resembles that of EHes. Excess of heavy metals (Y, Zr and Ba) is, however, not statistically significant. Note also very high abundance of Ne in LS IV-14°109 compared to KS Per at close metallicity of both stars.

Opposite to a pair of HdBs KS Per and ν Sgr, EHes are not binary systems and do not show the infrared excess. According to one popular scenario EHes could be produced by merging of a He white dwarf with a CO white dwarf. HdBs cannot be regarded as precursors of EHes as the mass of the components would be above the Chandrasekhar limit and rather a supernova event may result (Morrison 1988).

We revealed a complex emission + absorption profile of the Na I D and suggest that the emission component forms in the circumbinary gaseous envelope. To obtain more realistic interpretation of the Na I D doublet profile one needs both spectral monitoring and spectropolarimetry with high spectral resolution. Based on photoelectric polarimetric observations, Pfeiffer & Koch (1973) reported that KS Per possess significant and variable degree of polarization, $P = 1.84 \div 2.18\%$.

We have found that the luminosity of KS Per is $\log L/L_{\odot} \approx 3.3$ which together with $T_{\text{eff}} = 9500$ K corresponds to spectral type A2II. This is somewhat different from the result of direct spectral classification A5Iap (SIMBAD data base). Again, compared to ν Sgr with $M_V = -4.8 \pm 1.0$ (Kameswara Rao & Venugopal 1985) KS Per is less luminous.

ACKNOWLEDGEMENTS. This research was supported by the Estonian Science Foundation grant nr. 6810 (T. Kipper). V. Klochkova acknowledges support by the Russian Foundation for Basic Research (project 08-02-00072 a), the fundamental research program “Extended Objects in the Universe” of the Division of Physical Sciences of the Russian Academy of Sciences, and the program “Origin and Evolution of Stars and Galaxies” of the Presidium of the Russian Academy of Sciences.

This research has made use of the SIMBAD database, operated at CDS, Strasbourg France.

REFERENCES

- Artru M.C., Jamar C., Petrini D. & Praderie F. 1981, *A&A*, **44**, 171
 Asplund M., Gustafsson B., Lambert D.L. & Rao N.K. 2000, *A&A*, **353**, 287
 Asplund M., Grevesse N. & Sauval A.J. 2005, *ASP Conf. Ser.*, **336**, 25
 Bidelman W.P. 1950, *ApJ*, **111**, 333
 Biémont E. & Godefroid M. 1980, *A&A*, **84**, 361
 Dame T.M., Hartmann D. & Thaddeus P., 2001, *ApJ*, **547**, 792
 Danziger I.J., Wallerstein G. & Böhm-Vitense E. 1967, *ApJ*, **150**, 239
 Delgado A.J. & Thomas A.-C. 1981, *A&A*, **96**, 142
 Drilling J.S. & Schönberner D. 1982, *A&A*, **113**, L22
 Dudley R.E. & Jeffery C.S. 1990, *MNRAS*, **247**, 400
 Dudley R.E. & Jeffery C.S. 1993, *MNRAS*, **262**, 945
 Hakkila J., Myers J., Stidham B. & Hartmann D. 1997, *AJ*, **114**, 2043
 van Hoof P. 1999, <http://www.pa.uky.edu/~peter/atomic>
 Jardine K. 2008, <http://galaxymap.org/drupal/node/100>
 Jeffery C.S., Woolf V.M. & Pollaco D.L. 2001, *A&A*, **376**, 497
 Iben I.Jr. & Tutukov A.V. 1993, *ApJ*, **418**, 343
 Kameswara Rao N. & Venugopal V.R. 1985, *J. Ap. & A.*, **6**, 101
 Kipper T. & Klochkova V.G. 2005, *Baltic Astronomy*, **14**, 215
 Kipper T. & Klochkova V.G. 2006, *Baltic Astronomy*, **15**, 531
 Leushin V.V., Snezhko L.I. & Chuvenkov V.V. 1998, *Astron. Lett.*, **24**, 45
 Leushin V.V. 2001, *Astron. Lett.*, **27**, 643
 Lodders K. 2003, *ApJ*, **591**, 1220
 Margoni R., Stagni R. & Mammano A. 1988, *A&AS*, **75**, 157
 Munari U. & Zwitter T. 1997, *A&A*, **318**, 269
 Nariai K. 1963, *PASJ*, **15**, 449
 Nariai K. 1967, *PASJ*, **19**, 63
 Osawa K., Nishimura S. & Nariai K. 1963, *PASJ*, **15**, 313

- Panchuk V.E., Klochkova V.G., Najdenov I.D. & Yushkin M.V. 2007, *In: "UV Astronomy: Stars from birth to death"*, eds. A. I. de Castro & M. A Barstow. Madrid, UCM Editorial Complutense, 179
- Pandey G., Kameswara Rao N., Lambert D.L., Jeffery C.S. & Asplund M. 2001, MNRAS, **324**, 937
- Pandey G. 2006, ApJ, **648**, L143
- Parthasarathy M., Hack M. & Tektunali G. 1990, A&A, **230**, 136
- Parthasarathy M., Branch D., Jeffery D.J. & Baron E. 2007, astro-ph/0703415
- Pfeiffer R.J. & Koch R.H. 1973, IBVS, No. 780
- Thevenin F. 1989, A&AS, **77**, 137
- Thevenin F. 1990, A&AS, **82**, 179
- Timmes F.X., Woosley S.E. & Weaver T. 1995, ApJS, **98**, 617
- Uomoto A. 1986, ApJ, **310**, L35
- Wallerstein G., Greene T.F. & Tomley L.J. 1967, ApJ, **150**, 245
- Wheeler J.C., Sneden C. & Truran J.W. 1989, A&A, **27**, 279
- Wiese W.L., Fuhr J.R. & Deters T.M. 1996, J. Chem. Ref. Data, Mono. 7
- Zeldovich Ya.B. & Guseinov O.H. 1966, ApJ, **144**, 840

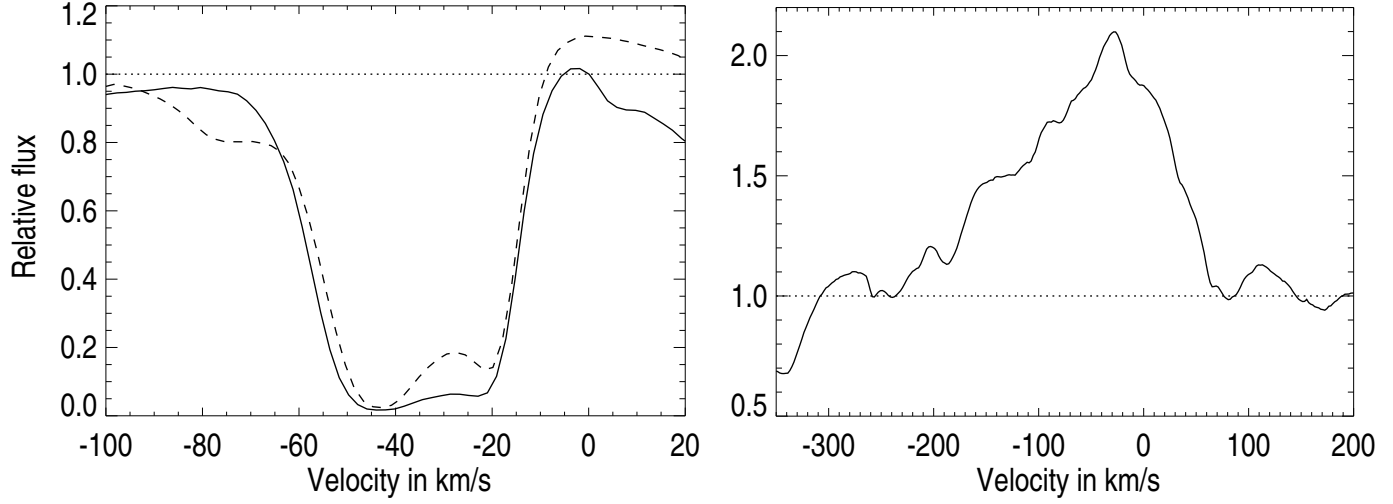


Fig. 1. The Na D doublet in the *KS Per* spectrum in velocity scale (left). The D₂ component is plotted with solid line, the D₁ with dashed line. For both components the red half of the line show P Cygni profiles, the blue component is also of CS origin. In the right panel the H α emission is depicted in velocity scale.

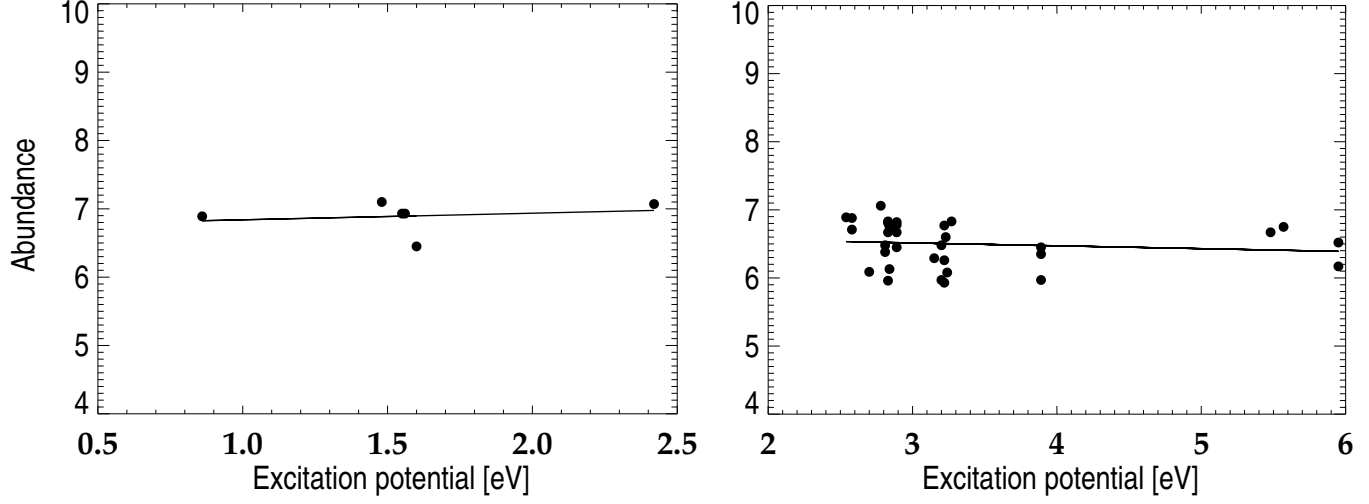


Fig. 2. The dependence of the iron abundance on the lower excitation potential of the used lines for Fe I (left) and Fe II (right). The hydrogen deficient model with $T_{\text{eff}} = 9500$ K and $\log g = 2.00$ together with micro-turbulent velocities 8.3 km s^{-1} for Fe I and 9.4 km s^{-1} for Fe II was used.

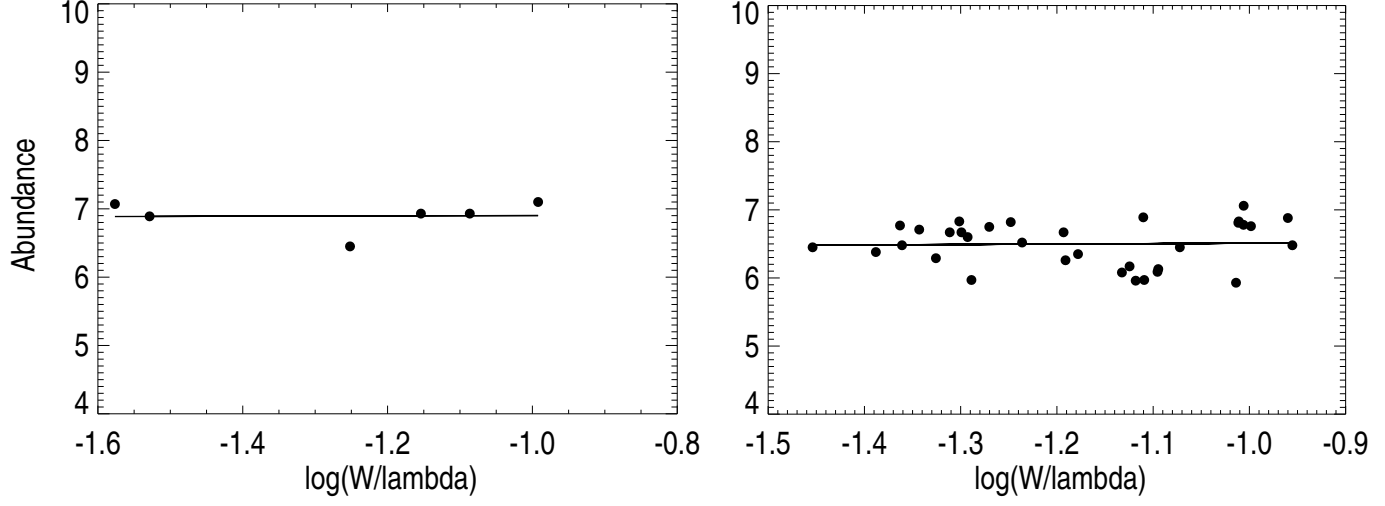


Fig. 3. The dependence of the iron abundance on W_λ/λ of the used lines for Fe I (left) and Fe II (right). The microturbulent velocities are 8.3 km s^{-1} for Fe I and 9.4 km s^{-1} for Fe II.

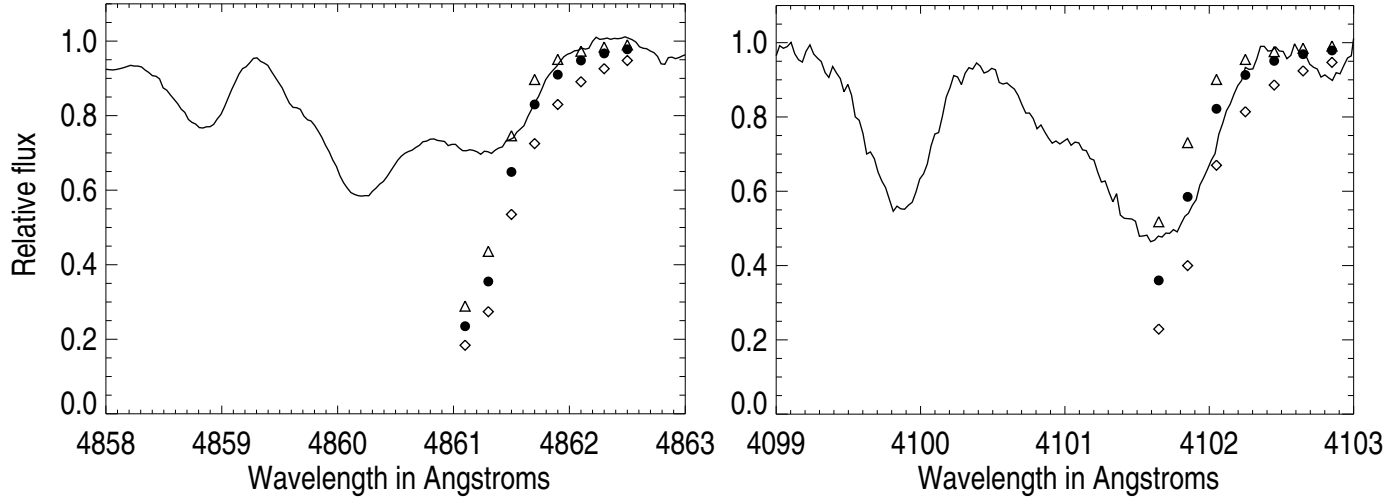


Fig. 4. The H β (left) and H δ (right) lines in the spectrum of KS Per. Solid line – the observed spectrum, triangles – calculated lines with $H/He = 10^{-5}$, filled circles – $H/He = 2 \cdot 10^{-5}$, diamonds – $H/He = 5 \cdot 10^{-5}$.

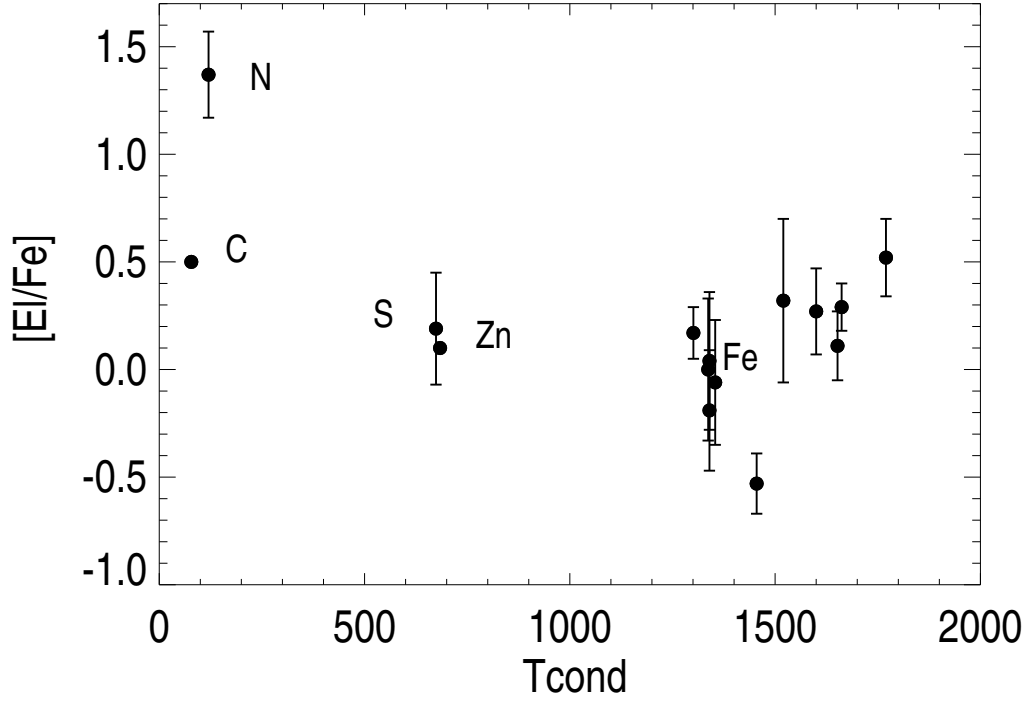


Fig. 5. The abundances of the elements in the atmosphere of *KS Per* versus their condensation temperature.

Table 1. Basic parameters of KS Per (SIMBAD database).

KS Per	=HD 30353
α_{2000}	04 48 53.35
δ_{2000}	43 16 32.10
Galactic coordinates l b	161.73 −01.01
Mean magnitude B	8.14
V	7.76
Spectral type	A5Iap
IRAS fluxes f_{12}	1.58
(Jy) f_{25}	0.52
f_{60}	0.40
f_{100}	1.35

Table 2. The chemical composition of *KS Per*. The abundances are normalised so that $\log \Sigma \mu_i \varepsilon(i) = 12.15$. In the Remarks the number of used lines and the source of oscillator strengths are indicated.

El.	Sun ¹	KS Per		Remarks
	$\log \varepsilon$	$\log \varepsilon$	[El/Fe]	
H	12.00	7.0		
He	10.93	11.54 ± 0.23		
C	8.39	8.1		Input abundance
N	7.78	8.36 ± 0.20	1.4	11 N I, 5 N II, WFD ²
O	8.66	7.72 ± 0.17	-0.2	3 O I, WFD
Ne	7.84	7.66 ± 0.14	0.6	8 Ne I, K ³
Mg	7.53	6.55 ± 0.28	-0.2	4 Mg I, T ⁴ , 7 Mg II, T, K
Si	7.51	6.76 ± 0.32	0.0	16 Si II, K, A ⁵
S	7.14	6.54 ± 0.26	0.2	7 S II, K
Sc	3.05	2.37 ± 0.16	0.1	3 Sc II, T
Ti	4.90	4.38 ± 0.20	0.3	19 Ti II, T
V	4.00	2.68 ± 0.14	-0.5	3 V II, T
Cr	5.64	5.02 ± 0.12	0.2	27 Cr II, T
Fe	7.45	6.66 ± 0.33		6 Fe I, 33 Fe II, T
Ni	6.23	5.38 ± 0.29	-0.1	3 Ni II, T
Sr	2.92	2.23 ± 0.09	0.1	2 Sr II, T
Y	2.24	1.74 ± 0.11	0.3	2 Y II, T
Zr	2.59	2.32 ± 0.18	0.5	5 Zr II, T
Ba	2.17	1.70 ± 0.38	0.3	3 Ba II, T

¹ Asplund et al. (2005), relative to $\log \varepsilon(\text{H})$,

² Wiese et al. (1996),

³ Thevenin (1989, 1990),

⁴ van Hoof (1999),

⁵ Artru et al. (1981).

Table 3. The chemical abundances pattern of KS Per in comparison to that of the extreme helium star LS IV–14°109 (Pandey et al., 2001).

El.	$\log \varepsilon$		
	Sun	KS Per 9500 K, 2.0	LS IV–14°109 9500 K, 0.9
H	12.00	7.0	6.2
He	10.93	11.54	11.54
C	8.39	8.1	9.4
N	7.78	8.36	8.6
O	8.66	7.72	8.5
Ne	7.84	7.67	9.4
Mg	7.53	6.55	6.9
Si	7.51	6.76	7.8
S	7.14	6.54	7.6
Sc	3.05	2.37	3.3
Ti	4.90	4.38	4.3
Cr	5.64	5.02	5.1
Fe	7.45	6.66	6.8
Ni	6.23	5.38	6.6
Sr	2.92	2.23	2.6
Y	2.24	1.74	1.9
Zr	2.59	2.32	1.9
Ba	2.17	1.70	1.7

Table 4. Atomic data (wavelengths [nm], lower level excitation potentials ϵ_i [eV], oscillator strengths $\log gf$), equivalent widths [pm] and abundances calculated with the model parameters $T_{\text{eff}} = 9500$ K, $\log g = 2.0$ and $\xi_t = 9.5 \text{ km s}^{-1}$ for HD 30353.

El.	λ	ϵ_i	$\log gf$	EW	$\log \varepsilon$	El.	λ	ϵ_i	$\log gf$	EW	$\log \varepsilon$
He I	400.926	21.22	-1.45	45.1	0.12	Si II	407.678	9.84	1.55	36.	-4.28
He I	402.926	20.96	-0.47	60.0	-0.07	Si II	437.697	12.84	-0.84	24.4	-4.28
He I	414.376	21.22	-1.20	47.7	0.06	Si II	467.328	12.84	-0.39	22.7	-4.83
He I	492.193	21.22	-0.44	52.3	-0.31	Si II	469.314	12.15	-1.74	7.0	-4.78
He I	504.774	21.22	-1.60	44.2	0.39	Si II	477.430	12.84	-1.84	7.9	-4.29
						Si II	484.479	12.88	-1.36	6.7	-4.84
N I	409.950	12.01	-1.46	24.1	-2.80	Si II	546.215	12.87	-1.02	14.2	-4.67
N I	410.995	10.69	-1.23	34.5	-3.22	Si II	546.946	12.88	-0.72	17.9	-4.75
N I	599.943	11.60	-1.11	22.6	-3.49	Si II	557.597	12.88	-1.25	13.3	-4.48
N I	600.847	11.60	-1.41	25.0	-3.09	Si II	568.886	14.17	0.08	14.7	-5.08
N I	664.650	11.75	-1.54	17.0	-3.22	Si II	570.138	14.17	-0.10	13.0	-5.02
N I	665.346	11.75	-1.14	26.3	-3.26	Si II	580.050	14.49	-0.17	16.3	-4.58
N I	561.654	11.71	-1.32	22.2	-3.23	Si II	597.893	10.07	-0.04	44.2	-5.50
N I	562.320	11.71	-1.60	16.4	-3.19	Si II	634.711	8.12	0.18	88.5	-4.70
N I	581.650	11.83	-1.97	12.5	-2.93	Si II	637.137	8.12	-0.12	80.4	-4.75
N I	664.500	11.71	-0.91	29.5	-3.38	Si II	667.190	14.49	0.52	23.9	-4.82
N I	493.512	10.69	-1.89	19.2	-3.29						
N II	460.715	18.48	-0.51	8.3	-3.32	S II	426.776	16.10	0.30	16.2	-4.83
N II	461.387	18.48	-0.67	7.6	-3.22	S II	446.358	15.94	0.22	9.5	-5.24
N II	464.309	18.48	-0.36	10.4	-3.30	S II	448.343	15.90	-0.06	13.2	-4.71
N II	567.956	18.48	0.25	18.9	-3.13	S II	448.663	15.87	-0.46	7.6	-4.74
N II	637.962	18.47	-0.95	6.5	-2.78	S II	471.627	13.62	-0.22	18.7	-5.23
						S II	491.720	14.00	-0.33	12.0	-5.35
O I	533.073	10.74	-0.87	21.0	-4.08	S II	543.280	13.62	0.16	31.1	-4.85
O I	615.817	10.74	-0.30	39.6	-3.95	Sc II	424.684	0.31	0.36	47.0	-9.22
O I	543.577	10.74	-1.54	13.0	-3.77	Sc II	440.040	0.61	-0.28	36.2	-8.99
						Sc II	552.682	1.77	0.18	25.4	-9.30
Ne I	503.775	18.56	-0.82	4.8	-4.05						
Ne I	585.249	16.85	-0.49	19.9	-3.99	Ti II	402.835	1.89	-0.89	46.8	-6.83
Ne I	588.189	16.62	-0.77	20.9	-3.74	Ti II	428.789	1.08	-1.59	32.4	-7.50
Ne I	597.553	16.62	-1.27	10.9	-3.86	Ti II	431.680	2.05	-1.74	24.5	-7.05
Ne I	614.306	16.62	-0.10	30.4	-3.85	Ti II	433.071	1.17	-2.28	22.8	-7.11
Ne I	616.359	16.72	-0.62	21.0	-3.82	Ti II	434.137	1.12	-2.20	27.4	-7.07
Ne I	626.650	16.72	-0.30	26.8	-3.80	Ti II	442.194	2.06	-1.72	25.5	-7.05
Ne I	640.225	16.62	0.33	35.6	-3.92	Ti II	445.049	1.08	-1.47	39.2	-7.37
						Ti II	447.086	1.16	-2.21	30.6	-6.96
Mg I	470.299	4.35	-0.55	13.0	-4.55	Ti II	448.833	3.12	-0.65	35.6	-7.08
Mg I	516.733	2.71	-0.75	30.2	-4.78	Ti II	452.949	1.57	-1.72	28.3	-7.27
Mg I	517.270	2.71	-0.32	35.6	-5.02	Ti II	458.995	1.24	-1.64	43.2	-6.98
Mg I	518.362	2.72	-0.08	29.4	-5.47	Ti II	470.867	1.24	-2.38	19.3	-7.17
						Ti II	477.998	2.05	-1.50	21.6	-7.47
Mg II	439.057	10.00	-0.52	42.0	-4.96	Ti II	479.854	1.08	-2.74	17.1	-7.00
Mg II	442.799	10.00	-1.21	29.2	-4.96	Ti II	487.401	3.09	-1.01	28.5	-7.08
Mg II	443.399	10.00	-0.90	37.1	-4.86	Ti II	512.916	1.89	-1.27	35.0	-7.41
Mg II	448.133	8.86	0.74	65.9	-5.44	Ti II	526.215	1.58	-2.30	20.9	-7.06
Mg II	473.959	11.57	-0.42	31.1	-4.85	Ti II	533.679	1.58	-1.65	30.9	-7.40
Mg II	485.110	11.63	-0.42	34.5	-4.65	Ti II	538.103	1.57	-2.05	26.2	-7.16
Mg II	654.594	11.63	0.41	41.1	-5.30						

Table 4. Continued.

El.	λ	ϵ_i	$\log gf$	EW	$\log \varepsilon$	El.	λ	ϵ_i	$\log gf$	EW	$\log \varepsilon$
V II	403.561	1.79	-0.12	30.5	-8.86	Fe II	466.371	2.89	-4.06	29.9	-4.87
V II	430.110	4.02	0.68	14.5	-9.00	Fe II	466.675	2.83	-3.53	45.5	-4.71
V II	533.266	2.27	-1.06	8.6	-8.72	Fe II	512.035	2.83	-4.37	25.0	-4.87
						Fe II	513.267	2.81	-4.23	21.0	-5.16
Cr II	413.241	3.76	-2.35	29.4	-6.41	Fe II	523.463	3.22	-2.31	50.7	-5.61
Cr II	424.238	3.87	-1.11	50.3	-6.52	Fe II	525.693	2.89	-4.32	29.7	-4.72
Cr II	425.263	3.86	-2.00	34.7	-6.48	Fe II	528.411	2.89	-3.31	52.1	-4.76
Cr II	427.556	3.86	-1.45	41.5	-6.71	Fe II	532.556	3.22	-3.38	34.3	-5.28
Cr II	455.499	4.07	-1.53	45.5	-6.41	Fe II	533.773	3.23	-3.98	27.2	-4.94
Cr II	455.865	4.07	-0.67	61.0	-6.34	Fe II	536.287	3.20	-2.80	41.7	-5.57
Cr II	459.206	4.07	-1.51	47.2	-6.36	Fe II	540.882	5.95	-2.19	31.4	-5.02
Cr II	461.879	4.07	-1.21	48.1	-6.60	Fe II	552.514	3.27	-4.21	27.6	-4.71
Cr II	463.408	4.07	-1.25	51.5	-6.39	Fe II	553.485	3.24	-2.96	40.8	-5.46
Cr II	481.235	3.86	-1.99	36.4	-6.55	Fe II	581.367	5.57	-2.69	31.2	-4.79
Cr II	482.414	3.87	-0.94	57.4	-6.55	Fe II	599.138	3.15	-3.76	28.3	-5.25
Cr II	483.624	3.86	-2.18	39.7	-6.23	Fe II	608.410	3.20	-3.99	26.5	-5.06
Cr II	486.022	3.87	-2.21	35.2	-6.40	Fe II	611.333	3.22	-4.26	26.5	-4.77
Cr II	486.432	3.86	-1.50	51.8	-6.35	Fe II	614.774	3.89	-2.92	40.8	-5.19
Cr II	487.640	3.85	-1.68	42.5	-6.62	Fe II	623.350	5.48	-2.70	31.3	-4.87
Cr II	488.460	3.86	-2.24	30.3	-6.58	Fe II	624.756	3.89	-2.55	52.9	-5.09
Cr II	524.678	3.71	-2.55	23.0	-6.67	Fe II	636.946	2.89	-4.31	22.4	-5.09
Cr II	524.942	3.76	-2.64	24.0	-6.51	Fe II	641.693	3.89	-2.86	33.0	-5.57
Cr II	527.498	4.07	-1.55	44.4	-6.63						
Cr II	530.843	4.07	-2.07	33.5	-6.57	Ni II	401.504	4.03	-2.44	38.5	-5.98
Cr II	531.070	4.07	-2.34	29.0	-6.45	Ni II	424.480	4.03	-3.02	28.2	-6.00
Cr II	531.359	4.07	-1.78	35.5	-6.77	Ni II	436.210	4.03	-2.34	32.3	-6.49
Cr II	533.776	4.07	-2.18	30.0	-6.59						
Cr II	540.762	3.83	-2.38	28.0	-6.61	Sr II	407.772	0.00	0.17	41.1	-9.39
Cr II	542.093	3.76	-2.49	28.6	-6.52	Sr II	421.554	0.00	-0.38	34.4	-9.22
Cr II	550.863	4.15	-2.20	30.0	-6.54						
Cr II	605.347	4.73	-2.18	19.9	-6.62	Y II	417.754	0.41	0.20	25.2	-9.67
						Y II	430.963	0.18	-0.42	11.6	-9.76
Fe I	404.582	1.48	0.29	41.2	-4.68	Y II	437.494	0.41	0.30	26.6	-9.75
Fe I	406.361	1.55	0.00	33.3	-4.75						
Fe I	407.175	1.60	-0.04	22.8	-5.12	Zr II	414.920	0.80	0.08	22.9	-9.46
Fe I	429.925	2.42	-0.72	11.4	-4.46	Zr II	420.899	0.71	-0.51	20.5	-9.04
Fe I	440.476	1.56	-0.25	30.9	-4.70	Zr II	421.190	0.53	-0.65	19.2	-9.06
Fe I	526.955	0.86	-1.42	15.6	-4.65	Zr II	435.974	1.24	-0.25	12.5	-9.30
						Zr II	449.697	0.71	-0.85	9.3	-9.22
Fe II	412.267	2.58	-3.53	45.2	-4.66						
Fe II	412.479	2.54	-4.26	32.0	-4.65	Ba II	455.404	0.00	0.93	23.7	-10.36
Fe II	427.333	2.70	-3.31	34.3	-5.45	Ba II	493.409	0.00	-0.10	16.0	-9.68
Fe II	436.941	2.78	-3.82	43.1	-4.48	Ba II	614.173	0.70	0.27	23.0	-9.48
Fe II	448.918	2.83	-3.15	34.2	-5.58						
Fe II	452.023	2.81	-2.88	50.1	-5.06						
Fe II	457.634	2.84	-3.22	36.8	-5.41						
Fe II	458.283	2.84	-3.41	46.0	-4.78						
Fe II	462.052	2.83	-3.52	45.0	-4.73						
Fe II	463.531	5.95	-1.60	34.8	-5.37						
Fe II	464.895	2.58	-4.62	21.1	-4.83						